https://doi.org/10.5194/essd-2026-791
Preprint. Discussion started: 9 November 2026
© Author(s) 2026. CC BY 4.0 License.



Open Access Earth System Science Data Discussions

Annual global terrestrial ecosystem maps from 1982 to 2024 aligned with the IUCN Global Ecosystem Typology

Zhenrong Du[1], Le Yu[2,3,4], Xiyu Li[2], Hui Wu[5], Ruyue Chang[1], Alice C. Hughes[6], David Coomes[7], James G.C. Ball[7], Xiaorui Ma[1], Hongyu Wang[1], Huawei Wan[8], Jixi Gao[8], and Keping Ma[5,9]

1 School of Information and Communication Engineering, Dalian University of Technology, Dalian 116024, China
2 Department of Earth System Science, Ministry of Education Key Laboratory for Earth System Modeling, Institute for Global Change Studies, Tsinghua University, Beijing 100084, China
3 Ministry of Education Ecological Field Station for East Asian Migratory Birds, Department of Earth System Science, Tsinghua University, Beijing 100084, China
4 Institute of Carbon Neutrality, Tsinghua University, Beijing 100084, China
5 Northeast Asia Biodiversity Research Center, College of Forestry, Northeast Forestry University, Harbin 150040, China
6 School of BioSciences, University of Melbourne, Royal Parade, Parkville, VIC 3010, Australia
7 Conservation Research Institute and the Department of Plant Sciences, University of Cambridge, CB2 3EA Cambridge, U.K.
8 Center for Satellite Applications on Ecology and Environment, Ministry of Ecology and Environment, Beijing 100101, China
9 State Key Laboratory of Vegetation and Environmental Change, Institute of Botany, Chinese Academy of Sciences, Beijing 100093, China

Correspondence to: Le Yu (leyu@tsinghua.edu.cn)

Abstract. Spatially explicit and temporally consistent ecosystem data are needed for biodiversity assessment, ecosystem accounting, conservation planning, and Earth system analysis. Existing global products commonly provide either annual land cover without a functional ecosystem classification or ecosystem maps for a single reference period. In this research, we present annual global terrestrial ecosystem maps for 1982-2024 aligned with the IUCN Global Ecosystem Typology. The workflow combines annual land cover developed by Global Land Cover Change Monitoring Platform (FROM-GLC Plus) with 18 climate regions and four landform classes to define 507 World Terrestrial Ecosystem (WTE) types. These types are aggregated as fractions within 1 km grid cells and assigned to 41 terrestrial ecosystem functional groups (EFGs), together with three cross-realm categories, through an explicit rule-based crosswalk supported by indicative distribution maps and ancillary data. Validation used a pool of 100,500 globally distributed reference locations interpreted at the EFG level. Across the valid annual subsets for 1985-2024, overall accuracy ranged from 84.62 ± 0.55 % to 87.18 ± 0.40 %, with a mean of 86.14 ± 0.47 %. This dataset serves as a crucial resource for improving our understanding of long-term global terrestrial ecosystem dynamics, supporting biodiversity assessment and ecosystem accounting, informing conservation planning and policy decisions, and advancing Earth system research. The full archive of global annual EFGs is available at: https://doi.org/10.5281/zenodo.19448555 (Du et al., 2026).

https://doi.org/10.5194/essd-2026-791
Preprint. Discussion started: 9 November 2026
© Author(s) 2026. CC BY 4.0 License.



Open Access Earth System Science Data Discussions

1 Introduction

Terrestrial ecosystems form the living fabric of the Earth's surface, sustaining biodiversity, regulating carbon and water cycles, buffering climatic extremes, and providing the essential resources and services that support human livelihoods and health (Richardson et al., 2023). Over the past half century, the terrestrial biosphere has experienced unprecedented structural and functional reorganization under the combined pressures of land-use intensification and climate change (Conradi et al., 2024; Theobald et al., 2025). International frameworks, including the Millennium Ecosystem Assessment (Carpenter et al., 2006), the Kunming-Montreal Global Biodiversity Framework (CBD, 2024), and the UN Sustainable Development Goals (Colglazier, 2015), have emphasized the urgent need to monitor both the composition and condition of ecosystems as part of global environmental governance (Affinito et al., 2025). Yet despite the proliferation of regional studies and global indicators, a consistent, observation-based understanding of how terrestrial ecosystems are changing remains elusive.

Existing global mapping frameworks have provided valuable insights but remain unstandardised in how they represent ecosystem structure and function (Meyer and Pebesma, 2022; Schmidt-Traub, 2021). Traditional land-cover products, such as MODIS (Sulla-Menashe et al., 2019), ESA CCI (ESA, 2017) and the FROM-GLC (Gong et al., 2013), reflect the physical characteristics of the land surface but do not explicitly represent the ecological processes and functional roles that define ecosystems. In parallel, typological frameworks such as the IUCN Global Ecosystem Typology have established a unifying, function-based classification that links ecosystem structure, processes and environmental setting, and now serve as an important global reference for research, assessment and policy (Keith et al., 2022). However, the gap between high-resolution land-cover observations and conceptually robust ecosystem typologies has constrained our ability to track ecosystem degradation and recovery consistently, evaluate resilience across functional groups and attribute observed changes to biophysical or anthropogenic drivers (Bousfield and Edwards, 2025).

Bridging this divide requires an approach that unifies high-resolution, time-explicit remote sensing with a functional classification system grounded in ecological theory (Cavender-Bares et al., 2022). Recent advances in multi-source satellite data fusion and machine learning now make it possible to map global land cover annually (Zhang et al., 2024), while the IUCN typology provides a hierarchical structure capable of harmonizing diverse ecosystems across realms and biomes (Nicholson et al., 2024). Integrating these advances allows ecosystem monitoring to move from static inventories toward dynamic, observation-based systems that link type, function, and condition (Zeng et al., 2022). Such integration is essential for a critical step beyond previous approaches, such as those under the Aichi Biodiversity Targets, to support targeted ecological management with timely and spatially explicit monitoring of ecosystem dynamics.

Building on the IUCN Global Ecosystem Typology, recent efforts to map ecosystem functional groups (EFGs) globally have broadly followed two complementary strategies. The first translates a globally consistent environmental stratification and land cover maps into framework. Sides et al. (2025), for example, crosswalked the 2015 World Terrestrial Ecosystems (WTE) map to the IUCN typology. The WTE framework combines climate regions, landforms, and vegetation or land cover

https://doi.org/10.5194/essd-2026-791
Preprint. Discussion started: 9 November 2026
© Author(s) 2026. CC BY 4.0 License.



to define 1,781 biogeographically stratified ecosystem units at 250 m resolution. Each WTE unit was then assigned to its most probable EFG on the basis of similarities in climate, terrain, vegetation, terminology, and geographic distribution, resulting in a global map of 41 terrestrial EFGs. A second strategy is to synthesize existing ecosystem maps directly. The Global Ecosystems Atlas follows this approach by discovering and evaluating available local, national, and regional ecosystem maps, cross-referencing eligible classes to the IUCN Global Ecosystem Typology, harmonizing them into a 100-m synthesis product, and using spatial models to fill geographic gaps. It also incorporates the EcoTrain occurrence dataset, records pixel-level provenance and areas of disagreement, and emphasizes open licensing, metadata, and interoperability (Murray et al., 2026).

These two strategies offer different but complementary advantages. The synthesis-based approach of the Global Ecosystems Atlas can make direct use of detailed local and national ecosystem knowledge and preserve information that may not be captured by a globally uniform model, but its consistency and temporal coverage inevitably depend on the availability, update frequency, and compatibility of the contributing maps. In contrast, the environmentally stratified approach used by Sides et al. (2025) provides a globally consistent and reproducible framework that can be readily updated when new land-cover observations become available, although the crosswalk between stratified ecosystem units and EFGs is not always one-to-one and some assignments remain inherently uncertain. This ability to update EFG distributions using a consistent set of environmental strata is particularly valuable for global ecosystem monitoring. When coupled with annually updated land-cover observations, the framework can move EFG mapping beyond a static representation of ecosystem distribution toward a temporally continuous record, enabling rapid detection of ecosystem transitions, consistent comparison of change among functional groups, and long-term assessment of ecosystem dynamics at the global scale.

Therefore, here we describe annual global terrestrial ecosystem maps for 1982-2024 that connect a temporally consistent land-cover record to the GET. Following the environmental stratification used by the WTE framework, annual global land cover is mapped with improved Global Land Cover Change Monitoring Platform (FROM-GLC Plus), and then be combined with 18 climate regions and four landform classes to generate 507 WTE types. An explicit crosswalk then assigns these types to EFGs using the IUCN indicative distributions, the WTE map, plantation data, and expert rules. Potential ecosystem types and EFGs are reported as fractional areas within a common 1 km grid so that mixed composition is retained. The paper is organized following the data-production sequence: Section 2 describes the mapping and evaluation datasets, Section 3 documents the mapping and validation methods, Section 4 presents the data records and validation results, and Section 5 discusses their relation to existing ecosystem maps, recommended uses, and limitations.

2 Datasets

2.1 Mapping datasets

Annual land-cover maps for 1982–2024, produced using the FROM-GLC Plus framework (Yu et al., 2022; Du et al., 2024; Yu et al., 2025), provided the time-varying component for ecosystem mapping. The framework combines multi-source

https://doi.org/10.5194/essd-2026-791
Preprint. Discussion started: 9 November 2026
© Author(s) 2026. CC BY 4.0 License.



Earth observation records, including Landsat TM/ETM+/OLI, AVHRR, MODIS, with the first all-season sample set (FAST) training sample set (Li et al., 2017) and temporal sample migration (Yu et al., 2022). The classification system contains cropland, forest, grassland, shrubland, wetland, tundra, impervious surface, bareland, snow and ice, and water. The original 30 m annual land-cover maps were aggregated to a 1 km grid, with the fractional coverage of each land-cover class calculated as its percentage of the total area within each 1 km grid cell.

Environmental setting was represented by global climate regions and Hammond landforms. The climate layer contains 18 regions formed from six temperature domains and three moisture domains following the World Ecosystems mapping framework (Sayre et al., 2020). Temperature domains were derived from WorldClim version 2 climate surfaces (Fick and Hijmans, 2017), while moisture domains distinguish moist, dry, and desert conditions using the aridity index. The global Hammond landform layer contains mountains, hills, plains, and tablelands (Karagulle et al., 2017). Crossing the 18 climate regions with the four landform classes produces 72 environmental settings. The target ecosystem classification system was IUCN Global Ecosystem Typology v2.1 (Keith et al., 2022). EFG profiles and indicative distribution maps supplied the functional definitions and broad biogeographic constraints used during crosswalking. The Spatial Database of Planted Trees version 2.0 supplied plantation distributions and planting-year information (Du et al., 2022; Richter et al., 2024).

Table 1. Mapping datasets used to produce the annual global terrestrial ecosystem maps.

Dataset	Period	Resolution	Role	Reference
World climate regions	Static	250 m	Temperature and moisture domains	Fick and Hijmans (2017); Sayre et al. (2020)
Hammond landforms	Static	250 m	Mountains, hills, plains, and tablelands	Karagulle et al. (2017)
IUCN EFG maps	Static	30 arc seconds (~1 km)	Target EFG definitions and distribution constraints	Keith et al. (2022)
Spatial Database of Planted Trees (SDPT)	1982-2024/ annually	30 m	Plantation distribution and planting year	Du et al. (2022); Richter et al. (2024)

2.2 Evaluation data

Evaluation was based on a pool of 100,500 globally distributed locations originating from the FAST reference sample set. These evaluation locations were entirely independent of the samples used to train the underlying land-cover classification models and were not used at any stage of model training. The original land-cover interpretations were reviewed against high-resolution satellite imagery and the IUCN indicative distributions to obtain EFG-level reference labels. The number of valid reference locations was presented in Table 2, the number varies by year because an observation was retained only when the available imagery and reference information supported an EFG interpretation for that date.

Table 2. Valid sample size for global terrestrial ecosystem functional group (EFG) maps.

Years	1985	1990	1995	2000	2001	2002	2003	2004
Sample size	10803	14234	16136	16885	16710	16825	16934	16940

https://doi.org/10.5194/essd-2026-791
Preprint. Discussion started: 9 November 2026
© Author(s) 2026. CC BY 4.0 License.

Years	2005	2006	2007	2008	2009	2010	2011	2012
Sample size	16963	16921	17205	16966	17230	17090	17063	16850
Years	2013	2014	2015	2016	2017	2018	2019	2020
Sample size	18347	20292	21452	21960	22238	22441	22475	22530
Years	2021	2022	2023	2024				
Sample size	22625	22717	22800	22887				

3 Methods

The global terrestrial ecosystem maps were developed under the IUCN ecosystem typology with six hierarchical levels using both a top-down and bottom-up structure (Keith et al., 2022). The global ecosystem types were firstly derived from the bottom-up FROM-GLC Plus mapping framework and USGS World Terrestrial Ecosystem (WTE) mapping system. Then the global terrestrial ecosystem functional groups (EFGs) were integrated with global ecosystem maps and top-down by subdivision of biomes and realms. Finally, EFGs are summarized as fractional areas within a common 1 km grid. This design preserves the annual signal from land cover while keeping the environmental context and crosswalk auditable.

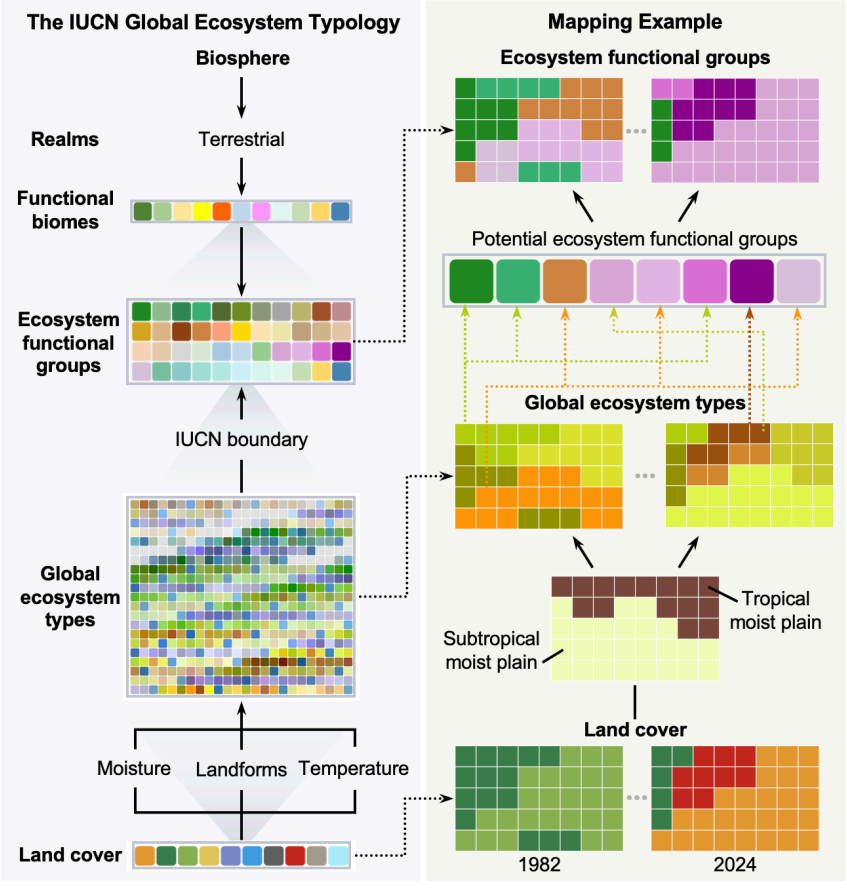


Figure 1. Hierarchical workflow for annual terrestrial ecosystem mapping within the IUCN Global Ecosystem Typology.

https://doi.org/10.5194/essd-2026-791
Preprint. Discussion started: 9 November 2026
© Author(s) 2026. CC BY 4.0 License.

Open Access Earth System Science Data Discussions

3.1 Annual land-cover mapping

As the foundational layer for global ecosystem mapping, we generated annual 30 m land-cover maps for 1982–2024 using the FROM-GLC Plus framework (Yu et al., 2022). The framework reconstructs temporally continuous observations by integrating Landsat TM, ETM+, and OLI imagery with MODIS and AVHRR data. MODIS MCD43A4 observations were used to fill temporal gaps after 2000, whereas AVHRR observations supported gap filling before 2000. Clouds and cloud shadows were removed using the quality-control information available for each sensor. The valid multi-source observations were then harmonized and smoothed to construct multispectral time series. For annual mapping, the observations were organized as mosaicked 16-day spectral time-series curves. Training data were derived from the FAST training sample set, which contains more than 91,000 locations. The original samples were collected in 2015, and we transferred FAST samples to each target year using the automatic sample-migration approach implemented in FROM-GLC Plus. For each sample, spectral angle distance (SAD) and Euclidean distance (ED) were calculated between its reference-period and target-year spectral features. A sample label was transferred only when both measures satisfied the predefined similarity thresholds, indicating that its spectral characteristics remained sufficiently stable.

For each target year, we constructed a feature matrix from six spectral bands and five spectral indices: blue, green, red, near-infrared, shortwave-infrared 1, shortwave-infrared 2, Normalized Difference Vegetation Index (NDVI), Enhanced Vegetation Index (EVI), Normalized Burn Ratio (NBR), Normalized Difference Built-up Index (NDBI), and Modified Normalized Difference Water Index (MNDWI). For each variable, we calculated the annual maximum, mean, standard deviation, and 25th, 50th, and 75th percentiles. A Random Forest classifier with 200 trees was trained using the migrated FAST samples for each year. The remaining classifier parameters followed the default settings in Google Earth Engine (GEE). Post-classification processing included temporal consistency checks and spatial filtering. The temporal checks were used to identify isolated annual class assignments that conflicted with the surrounding temporal trajectory, while spatial filtering reduced isolated pixels and salt-and-pepper noise. These procedures improved spatial and temporal consistency but may also remove genuine short-duration or small-area changes. The resulting maps followed the ten-class FROM-GLC classification system: cropland, forest, grassland, shrubland, wetland, tundra, impervious surface, bare land, snow and ice, and water. The workflow was implemented in GEE (Gorelick et al., 2017), allowing annual land-cover mapping at the global scale. We subsequently aggregated each 30 m annual map to a 1 km × 1 km reporting grid. For every grid cell, we calculated the fractional area occupied by each of the ten land-cover classes. These fractions, rather than only the dominant class, were retained as inputs for subsequent ecosystem mapping.

3.2 Construction of annual World Terrestrial Ecosystem (WTE)

We produced a new annual dataset of the WTE at 1 km resolution under the USGS classification system (Sayre et al., 2020) for the period of 1982-2024. Specifically, the global ecosystem dataset is a result of the systematic integration and objective development of three critical components: global climate regions, global landforms, and global land cover. This map offers

https://doi.org/10.5194/essd-2026-791
Preprint. Discussion started: 9 November 2026
© Author(s) 2026. CC BY 4.0 License.


a structured approach to understand the distribution of ecosystems across the globe.

In this study, the global climate regions layer (Sayre et al., 2020) was used to categorize the global climate into 18 distinct regions combined with six temperature regions and three moisture regions. To obtain temperature regions, the world temperature data was derived from WorldClim version 2 (Fick and Hijmans, 2017), which provides high-resolution climate data gathered from thousands of meteorological stations worldwide. The classification includes six temperature regions, with the addition of a subtropical domain to the IPCC's five temperature regions, enhancing alignment with global ecoregions. Then, world moisture domains divide global regions into three categories based on the aridity index (AI), humid ($AI > 0.65$), arid ($AI < 0.65$), and desert ($AI < 0.05$). Considering that it encompasses both precipitation and atmospheric water demand, this index stands out as a vital gauge for assessing moisture availability, particularly within the contexts of temperate, boreal, and polar climates (UNCCD, 2022). We then added the global landforms layer, a dataset that draws from the comprehensive global Hammond landforms (Karagulle et al., 2017). This layer categorizes the Earth's surface into four distinct classes: mountains, hills, plains, and tablelands. The classification system combined with the landforms layer expanded the 18 climate zone categories into 72 possible combinations, providing a more detailed representation of global ecological regions. Based on the ten land cover categories defined by FROM-GLC Plus, water, snow/ice, and tundra were treated as three independent classes, while the remaining seven categories were allocated into 72 possible combinations. In total, this framework yielded 507 WTE types. For the 1 km grid, the fractional area of each of the 507 ecosystem configurations was calculated based on the 30m land cover input, providing a sub-pixel estimate of ecosystem diversity.

3.3 Crosswalk to ecosystem functional groups

To achieve a consistent classification framework across realms, we developed a rule-based aggregation scheme that systematically assigned each mapped WTE unit to the most appropriate EFG within the Terrestrial, Freshwater–Terrestrial, and Freshwater domains based on the IUCN Global Ecosystem Typology v2.1 (Keith et al., 2022). This integration process was designed to reduce thematic redundancy and ensure comparability across spatial scales and ecological gradients.

Specifically, a rule-based aggregation framework was implemented to assign each WTE unit to its most appropriate EFG with Terrestrial, Freshwater-Terrestrial, and Freshwater realms. The rules combined multiple layers of information, including Spatial Database of Planted Trees (SDPT Version 2.0) (Richter et al., 2024), EFG indicative distribution maps, and WTE maps, as well as expert knowledge. F or terrestrial vegetation, we established an expert-informed crosswalk between each potential ecosystem type and up to 10 candidate EFGs, which are listed in descending order of suitability in Table S1. Candidate EFGs were ranked according to their concordance with the climate setting, landform, vegetation structure, land-cover characteristics, and biogeographic distribution of the source ecosystem type. The ranking also accounted for known thematic ambiguities in the source land-cover data, particularly among structurally similar or spectrally confusable classes such as grassland, shrubland, and bare land. Thus, alternative EFGs that could plausibly arise from these land-cover confusions were retained as lower-ranked candidates rather than being excluded a priori. This expert-informed crosswalking strategy is consistent with the approach of Sides et al. (2025), who assigned source ecosystem units

https://doi.org/10.5194/essd-2026-791
Preprint. Discussion started: 9 November 2026
© Author(s) 2026. CC BY 4.0 License.


to the most probable EFG on the basis of similarities in climate, terrain, vegetation, and geographic distribution, together with semantic concordance and apparent spatial overlap with the IUCN indicative EFG distribution maps. For each pixel, the ranked candidate EFGs were then evaluated sequentially. The highest-ranked candidate was assigned only when the pixel fell within the corresponding major or minor range of the EFG indicative distribution map; otherwise, the next-ranked candidate was evaluated, proceeding from EFG1 to EFG10. For example, ecosystems characterized as tropical moist montane forests were preferentially crosswalked to T1.3 Tropical/Subtropical Montane Rainforests, whereas warm temperate grasslands were preferentially assigned to T4.5 Temperate Tussock Grasslands, provided that the corresponding pixels occurred within the major or minor indicative ranges of those EFGs. Water-related ecosystems posed a particular challenge because of the difficulty in consistently distinguishing finer biomes of rivers and streams, lakes, artificial reservoirs (Lehner et al., 2024). To maintain coherence, all surface water units were therefore grouped into the broad Freshwater category, corresponding to the first-level class in the IUCN Global Ecosystem Typology, rather than subdividing into finer biomes and functional groups. Land-use intensive systems were handled separately. Cropland areas identified in the land-cover layers were directly assigned to T7.1 Croplands, while impervious surfaces were mapped to T7.4 Cities, Villages and Infrastructure. For plantation systems (T7.3 Plantations), we incorporated temporal information from SDPT V2 to reconstruct the distribution and planting years of tree plantations from 1982 to 2024. These annual plantation layers were integrated into the functional aggregation to provide year-specific representations of plantation extent.

This hierarchical mapping preserved ecological distinctiveness while providing a coherent global framework, which recognizes that WTE–EFG relationships are not strictly one-to-one; many-to-many associations and spatial overlaps among EFG maps are common (Keith et al., 2022). By combining explicit rules with expert knowledge and ancillary datasets, our aggregation ensures robust and spatially explicit assignments of ecosystems to functional groups, forming a critical foundation for subsequent ecological analyses. The final result is a global annual dataset which provides the fractional area coverage of each EFG within every 1 km ×1 km grid cell, resulting from the systematic calculation of the 507 ecosystem units composition at the 1 km scale. This approach provides a correspondence between each of the 507 ecosystem units and an EFG, forming a reproducible and scalable basis for ecosystem monitoring, change detection, and conservation assessment.

3.4 Accuracy and spatial plausibility assessment

To ensure the accuracy and reliability of the EFGs mapping results, we conducted an accuracy validation based on the independent validation samples from the FAST sample set, and assessed the accuracy of the 2024 map at 1-km scale. Specifically, we selected 100,500 globally distributed validation sample points, which cover various ecosystem types and represent the spatial heterogeneity of the global terrestrial surface. Since the original samples were interpreted based on land cover types, we performed a reinterpretation of the EFG type for these sample points, classifying them into the most appropriate EFG category. This reinterpretation process was developed with the constraints from IUCN EFG indicative distributions, and visual interpretation based on high-resolution satellite imagery, ensuring the accuracy and ecological

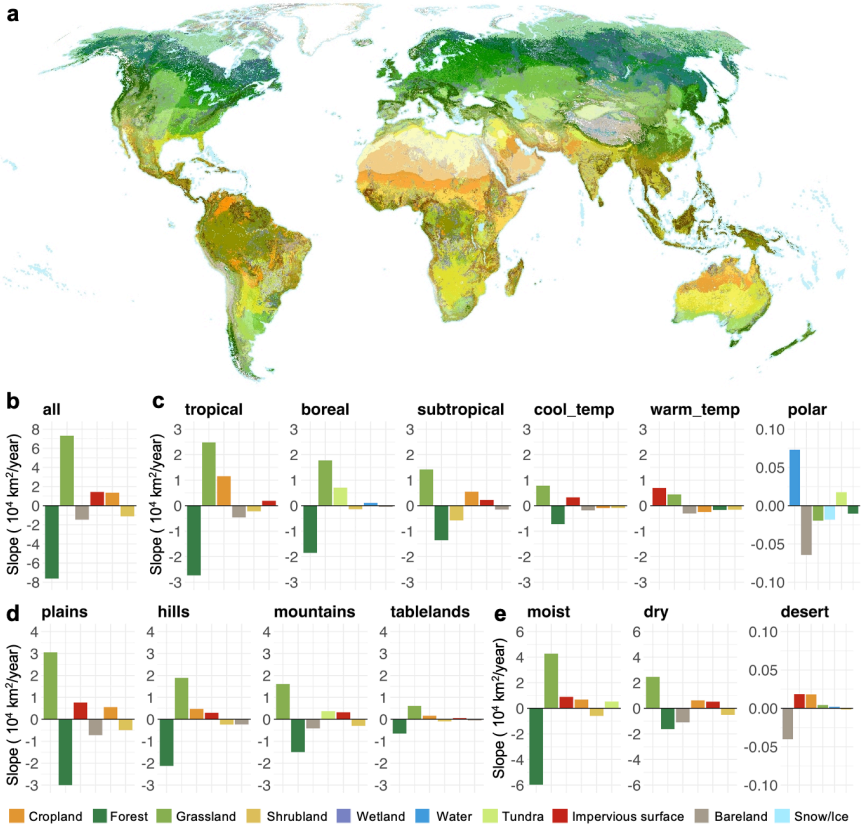
https://doi.org/10.5194/essd-2026-791
Preprint. Discussion started: 9 November 2026
© Author(s) 2026. CC BY 4.0 License.

231 rationality. Finally, we compared the classification results of our 1km EFG map at the sample points with the reinterpreted
232 reference labels, primarily using the Overall Accuracy (OA) and Kappa coefficient to quantify the accuracy of our global
233 EFG map. Additionally, the uncertainty of annual OA was estimated using an error matrix-based calibration estimator, with
234 95% confidence intervals calculated following Olofsson et al. (2014).

235 **4 Results**

236 **4.1 Annual global 30-m land cover and global ecosystem type maps**

237 Using annual 30-m FROM-GLC Plus land cover (Yu et al., 2022; Du et al., 2024; Yu et al., 2025), global climate regions,
238 and landforms, we generated annual global ecosystem maps for 1982–2024 that resolve 507 WTE types (Fig. 2a; Sayre et
239 al., 2020). By 2024, as shown in Table S2, the largest ecosystem type was Tropical Moist Forest on Plains (4.47 million
240 km²), while the smallest was Boreal desert Bareland on Plains (11.18 km²), aside from 70 marginal classes with <10 km².
241 Yet, only one-third of all classes (161 types) exceeded 100,000 km², and together they accounted for 97% of Earth's land
242 surface, while the remaining two-thirds were limited in extent and collectively accounted for less than 3%.



243

244 **Figure 2.** World Terrestrial Ecosystem (WTE) map and change analysis during 1982-2024. a) WTE map in 2024, the legend can be found
245 in Figure S1; the Theil-Sen slope estimates for the six land-cover classes with the largest absolute rates of change across b) all the
246 ecosystem types; c) temperature zones; d) landform units; e) moisture regimes.

https://doi.org/10.5194/essd-2026-791
Preprint. Discussion started: 9 November 2026
© Author(s) 2026. CC BY 4.0 License.



Over the past four decades, 10.55% of terrestrial ecosystems changed ecosystem type at least once. Theil–Sen trend analysis shows that forest loss (-7.63×10^4 km² yr^{-1}) and grassland expansion ($+7.32 \times 10^4$ km² yr^{-1}) dominate global land-cover transitions (Fig. 2b). These changes are most pronounced in humid plains and tropical regions (Fig. 2c–e), consistent with global land-change patterns in which forest loss and grassland expansion drive large-scale ecosystem restructuring. In warm, moist and plain regions, rapid expansion of settlements further accelerates the transformation from natural to human-dominated ecosystems (Fig. 2c–e). In cold and high-latitude regions, tundra and water have replaced snow/ice and bareland, signaling a functional shift of cryosphere-linked ecosystems under warming (Fig. 2c).

4.2 Annual global terrestrial ecosystem functional group

We produced annual global maps of terrestrial ecosystem functional groups (EFGs) from 1982 to 2024 by integrating global ecosystem types with the IUCN typology (Keith et al., 2022). The maps reflect consistent, spatially explicit trajectories of 41 EFGs across terrestrial realms and biomes, along with 3 realms (Freshwater, Marine-Terrestrial, and Marine-Freshwater-Terrestrial). Each annual map represents the proportional area of every EFG within a 1-km grid cell, enabling quantitative assessment of functional composition and its temporal dynamics at a globally consistent spatial scale.

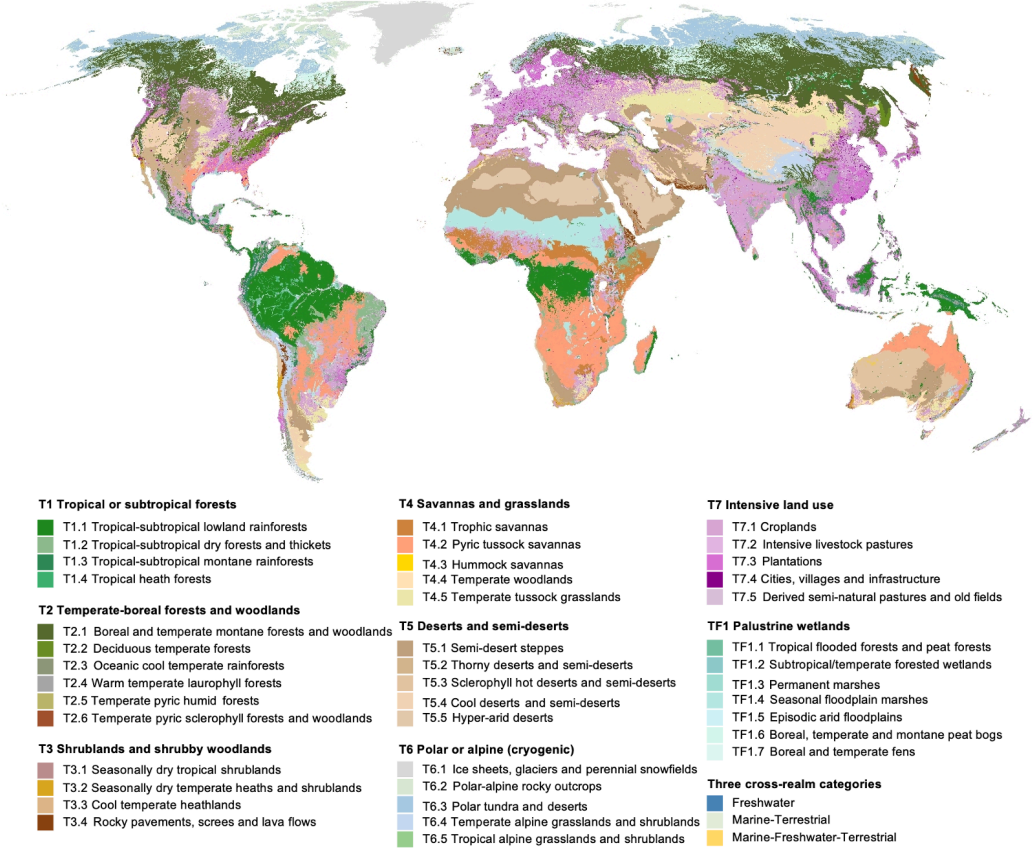


Figure 3. Global terrestrial ecosystem functional groups (EFGs) in 2024.

https://doi.org/10.5194/essd-2026-791
Preprint. Discussion started: 9 November 2026
© Author(s) 2026. CC BY 4.0 License.



The area-change trajectories across EFGs (Fig. 4a) highlight that most natural systems have contracted in area and that human-created EFGs dominate the expanding end of the spectrum. Between 1982 and 2024, the T1 Tropical–subtropical forest biome showed a total reduction of 11%, with T1.4 Tropical heath forests undergoing the sharpest contraction (−19%), indicating their vulnerability to deforestation and land-use intensification. The T2 Temperate boreal forests and woodlands biome declined in area by 13%, with T2.4 Warm temperate laurophyll forests showing the most pronounced decrease (−34%). In contrast, the T7 Intensive land-use systems biome displayed the most pronounced and directional transformation. T7.3 Plantations more than doubled in area, and T7.4 Cities, villages and infrastructure tripled, emerging as new structural anchors within the global functional network.

Functional transition patterns across EFGs over the past four decades (Fig. 4b) were spatially consistent with patterns of climate change and intensive human activity. Areas with the largest cumulative functional change are mainly concentrated in regions of intensive human activity, such as southeastern China and the United States, Southeast Asia, and Europe. In contrast, zones of high transition frequency, where pixels undergo multiple transitions between EFGs over time, often do not spatially coincide with areas of largest change. To further examine this decoupling, we conducted a Local Indicators of Spatial Association (LISA) analysis on transition frequency. For each grid cell, LISA compared its ecosystem transition frequency with those of its spatial neighbours, thereby identifying statistically significant local clusters and spatial outliers. High–high clusters represent cells with frequent transitions surrounded by similarly high-frequency cells, whereas high–low outliers indicate locally intense transitions embedded within relatively stable surroundings. Conversely, low–low clusters and low–high outliers identify spatially stable areas and locally stable cells within more dynamic landscapes, respectively. Spatially extensive high–high clusters typically occur in climate-sensitive regions experiencing large-scale, systemic transformation. For example, as shown in Figure S2, rapid warming, permafrost thaw, and widespread shrub expansion across the Arctic have reshaped vegetation composition, consistent with the functional-group transitions observed across permafrost regions in our dataset (Heijmans et al., 2022). Similarly, persistent shifts in precipitation regimes may contribute to the transition clusters associated with desertification, greening, and shrubification across central Asia, the Sahel, and inland Australia (Fig. 4b and Figure S2). In contrast, high–low spatial outliers may be more strongly associated with topography and localized human–environment interactions. These outliers occurred as linear belts along mountain ranges, river valleys, agro-pastoral ecotones, and coastal margins, or as isolated patches on islands. Notable examples include areas affected by China's large-scale afforestation projects within the agro-pastoral transition zone along the Hu Line (Chen et al., 2019) and forest loss within the well-documented Amazon arc of deforestation (Csillik et al., 2024). These spatial associations highlight locations where intense, localized restructuring of ecosystem functional groups coincides with strong anthropogenic pressures or pronounced ecological gradients.

https://doi.org/10.5194/essd-2026-791
Preprint. Discussion started: 9 November 2026
© Author(s) 2026. CC BY 4.0 License.

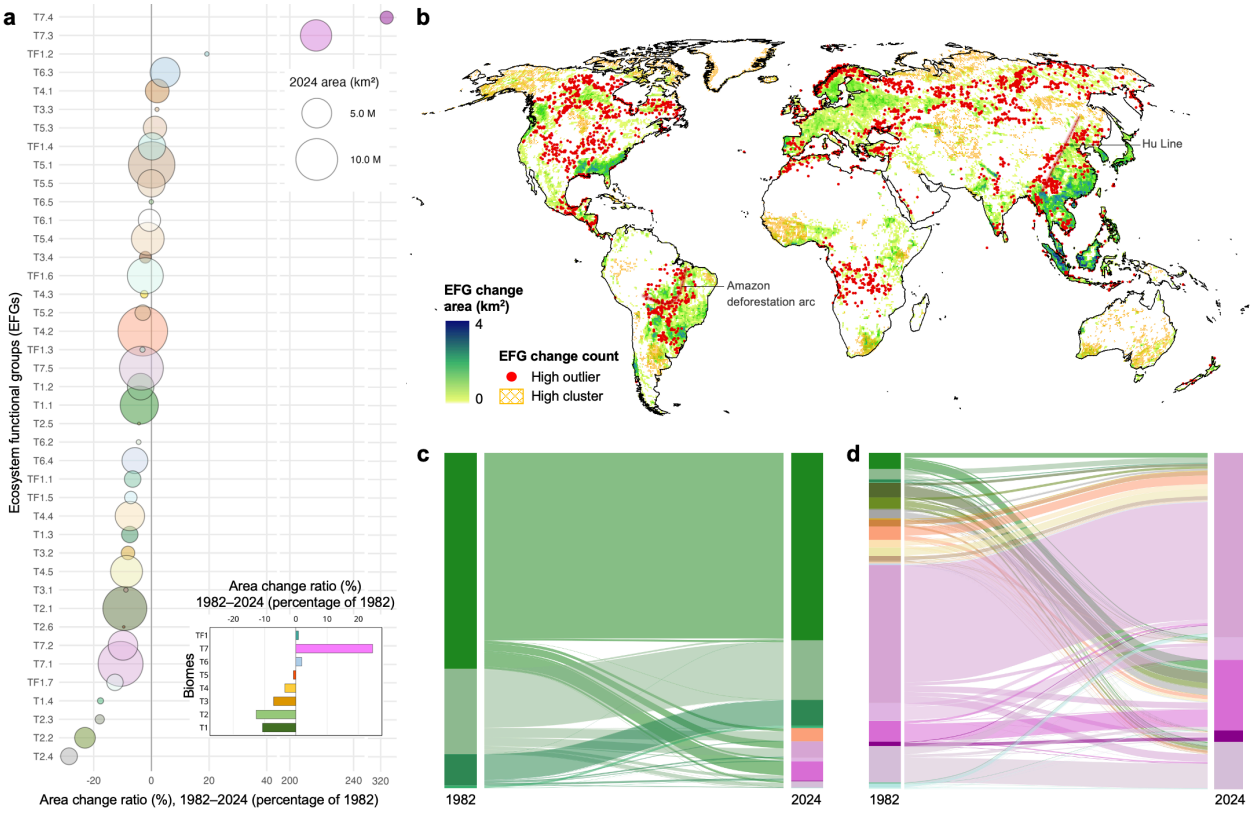


Figure 4. Global terrestrial ecosystem functional group (EFG) changes during 1982-2024. a) Percentage area change of each terrestrial EFG; b) EFG change area and local indicators of spatial association analysis for EFG change count; sankey diagram depicting area transition flows for c) the loss of T1 Tropical–subtropical forests and d) gain of T7 Intensive land-use systems.

The global transition matrix (Fig. S3) further reinforces the dominant roles of land-use intensification and desertification. T7 Intensive land-use systems overwhelmingly dominate the transition inflow, accounting for 46% of total area gained. On the outflow side, T2 Temperate–boreal forests and T4 Savannas and grasslands serve as primary donor biomes, contributing 24% and 19% respectively. Notably, T7 also exhibits a high outflow share (21%), reflecting the inherent instability and turnover of anthropogenic ecosystems (Riggio et al., 2020). Fig. 4c and 4d exemplifies these patterns by contrasting typical donor and recipient biomes. T1 Tropical–subtropical forests are frequently converted to tropical grasslands, croplands, and plantations. T7 systems are predominantly sourced from tropical and temperate forests and grasslands, while also showing substantial internal turnover, particularly transitions from croplands to other EFGs (Asamoah et al., 2021; Franco et al., 2025).

4.3 Accuracy assessment and evaluation

The resulting 1982–2024 EFG maps achieve an average OA of 86.14±0.47% and average Kappa coefficient of 0.83, confirming its robustness for global-scale assessment (Table 3). The terrestrial EFGs delineated under the IUCN typology

https://doi.org/10.5194/essd-2026-791
Preprint. Discussion started: 9 November 2026
© Author(s) 2026. CC BY 4.0 License.



Open Access Earth System Science Data Discussions

capture clear biogeographic patterns and structural transitions across realms and biomes. Building on the IUCN reference products that provide spatial benchmarks for global ecosystem distribution, our maps extend this framework to wall-to-wall, annually updated coverage for the full period 1982–2024, enabling dynamic tracking of ecosystem functional trajectories through time. This enables detection of both gradual and abrupt transitions in ecosystem states, while maintaining global consistency with the IUCN typology. A regional comparison (Figure 5) demonstrates the added value of our approach.

Table 3. Annual overall accuracy (OA) for global terrestrial ecosystem functional group (EFG) maps.

Years	**1985**	**1990**	**1995**	**2000**	**2001**	**2002**	**2003**	**2004**
OA (%)	85.43±0.63	84.62±0.55	84.81±0.51	85.41±0.49	85.34±0.50	85.67±0.49	85.66±0.49	85.95±0.49
Kappa	0.81	0.81	0.82	0.83	0.83	0.82	0.83	0.83
Years	**2005**	**2006**	**2007**	**2008**	**2009**	**2010**	**2011**	**2012**
OA (%)	85.85±0.49	85.98±0.49	85.98±0.48	86.14±0.48	86.31±0.48	86.52±0.48	86.51±0.48	86.72±0.48
Kappa	0.83	0.83	0.84	0.84	0.84	0.84	0.84	0.84
Years	**2013**	**2014**	**2015**	**2016**	**2017**	**2018**	**2019**	**2020**
OA (%)	86.92±0.45	86.06±0.46	86.47±0.42	86.37±0.43	86.50±0.42	86.34±0.43	86.44±0.42	86.50±0.42
Kappa	0.84	0.83	0.84	0.83	0.83	0.83	0.83	0.83
Years	**2021**	**2022**	**2023**	**2024**	**AVG**			
OA (%)	86.62±0.41	86.75±0.41	86.81±0.41	87.18±0.40	86.14±0.47			
Kappa	0.84	0.84	0.84	0.84	0.83			

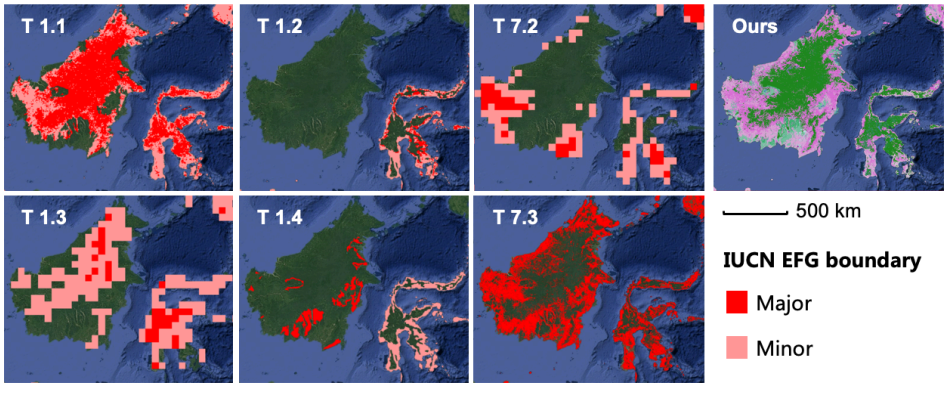


Figure 5. Global terrestrial ecosystem functional group map compared with IUCN reference boundaries. Background satellite imagery © Google Earth.

5 Discussion

5.1 Relation to existing global ecosystem maps

Our annual EFG maps show spatial agreement with existing global ecosystem products, including the Global Ecosystems Atlas (Murray et al., 2026) and the USGS crosswalk of the World Terrestrial Ecosystems (WTE) map (Sides et al., 2025). Major ecosystem patterns and regional boundaries are generally consistent among the products, indicating that

https://doi.org/10.5194/essd-2026-791
Preprint. Discussion started: 9 November 2026
© Author(s) 2026. CC BY 4.0 License.


the annual mapping framework captures the dominant spatial organization of terrestrial ecosystem functional groups. The comparison with the Global Ecosystems Atlas (Figure S3) highlights the strength of its synthesis-based approach in representing fine-scale ecosystem heterogeneity. By integrating national, regional, and global ecosystem maps together with locally informed information, the Atlas provides a more detailed representation of ecosystem patterns, particularly in coastal and transitional environments. Our product does not further subdivide Marine-Terrestrial, and Marine-Freshwater-Terrestrial ecosystems and therefore provides a simpler representation in coastal zones, where the Atlas distinguishes marine and coastal ecosystem types.

Agreement with the USGS WTE-to-EFG crosswalk is generally stronger (Fig. S4), which is expected because the two products follow similar environmental-stratification principles. Both combine land-cover information with climatic and landform constraints before translating the resulting ecosystem units into the IUCN Global Ecosystem Typology. Nevertheless, regional differences remain, largely because different land-cover datasets and ancillary information are used. In particular, our framework incorporates plantation information from the SDPT V2 dataset, allowing plantation ecosystems to be distinguished more explicitly from surrounding natural forests. This is especially evident in the southeastern United States, where large plantation-dominated areas are represented more clearly in our product. Generally, the three products are complementary. The Global Ecosystems Atlas provides greater local and thematic detail for current ecosystem distributions, whereas the USGS crosswalk offers a globally consistent reference based on environmental stratification. Our product builds on the latter concept while extending it through annually updated land-cover observations, providing a temporally continuous and internally consistent record of terrestrial EFG distributions over four decades. This combination makes it particularly suitable for analyses of ecosystem transitions, long-term change, and global ecosystem monitoring.

5.2 Limitations and uncertainty

Three main sources of uncertainty affect the EFG products. First, land-cover classification errors propagate through the workflow and influence the resulting ecosystem assignments. Second, climate regions and landforms impose discrete boundaries on environmental gradients that are continuous in nature. Third, the crosswalk combines ancillary distribution data with expert-defined rules, and some WTE types have multiple plausible EFG assignments. The IUCN indicative EFG distributions are used only as spatial priors to constrain the set of candidate EFGs. They represent broad distribution envelopes rather than precise ecosystem boundaries and are not treated as independent pixel-level reference data or ground truth. Consequently, the resulting products inherit the spatial uncertainty, variable source quality, and incomplete coverage of these indicative distributions. Ecosystem occurrences outside the mapped envelopes may be omitted, while broad or inaccurate envelopes may contribute to erroneous EFG assignments. Uncertainty in the plantation layers represents an additional limitation. SDPT V2 integrates datasets that differ among countries in plantation definitions, acquisition dates, completeness, and classification accuracy. These differences can produce regional underestimation or overestimation and may introduce artificial temporal inconsistencies into the reconstructed annual layers. Where planting-year information is used, the reconstruction may better represent documented plantation establishment than subsequent plantation loss,

https://doi.org/10.5194/essd-2026-791
Preprint. Discussion started: 9 November 2026
© Author(s) 2026. CC BY 4.0 License.


abandonment, conversion, or restoration to natural forest. Changes in mapped plantation extent should therefore not be interpreted as precise estimates of annual plantation expansion or contraction. Regional comparisons involving plantations require particular caution, especially where the underlying SDPT V2 coverage is incomplete or based on older source data.

Some thematic classes are also necessarily generalized because the source land-cover data do not distinguish all ecosystem categories represented in the Global Ecosystem Typology. The broad Freshwater class primarily represents surface-water areas that could not be assigned reliably to more specific aquatic or transitional EFGs. It may therefore include rivers, streams, lakes, reservoirs, etc. Similarly, assigning cropland-dominated pixels to T7.1 may combine annual herbaceous croplands with woody crops and rice paddies. Some of these systems would correspond to different EFGs if crop type, management, and hydrological information were consistently available. These generalizations may overestimate T7.1 and the broad Freshwater class while underrepresenting plantations and managed freshwater ecosystems.

For the reported areas in this study, they are map-based area estimates derived from classified pixels or fractional EFG cover. They should not be interpreted as unbiased estimates of true ecosystem extent. Classification errors can bias area estimates, particularly for rare EFGs and for classes with substantial omission or commission errors. Estimates of small gains, losses, and transitions are especially sensitive because classification errors may be comparable to the mapped changes. Probability-based reference sampling and error-adjusted area estimation would provide a more rigorous assessment, but these were not available for the present analysis. The direction and magnitude of the resulting area bias therefore remain unquantified. We consequently report area estimates with reduced numerical precision and interpret small differences cautiously.

5.3 An operational framework for dynamic terrestrial ecosystem monitoring

This study provides the first annual, reconstruction of global terrestrial ecosystems from 1982 to 2024 with the IUCN typology to generate dynamic EFGs, and evaluating long-term condition trajectories. By linking structure, function, and condition, we establish an operational framework for monitoring global ecosystems that moves beyond static inventories to dynamic, observation-based assessment.

Within this framework, the integration of multi-source remote sensing data, and cloud-based computation on Google Earth Engine enables global, annual, fine-scale mapping that was previously infeasible. Moreover, by adopting the IUCN's function-based EFG typology (Keith et al., 2022), our approach leverages a classification system that is both mechanistic and scalable, grounded in ecosystem traits rather than vegetation appearance or species composition alone. This typology simultaneously accommodates bottom-up compatibility with diverse land-cover datasets, while its hierarchical organization supports top-down consistency in global ecosystem zoning, making it inherently adaptable to climate-driven redistribution and suitable for multi-scale monitoring under future data refinements. Furthermore, our dynamic mapping approach demonstrates the feasibility and potential of near-real-time ecosystem monitoring based on FROM-GLC Plus (Yu et al., 2022; Du et al., 2024; Yu et al., 2025). As intra-annual land-cover updates become more frequent, abrupt disturbances such as fires, deforestation events and drought shocks can be detected within monthly or even daily time windows (Song, 2023).

https://doi.org/10.5194/essd-2026-791
Preprint. Discussion started: 9 November 2026
© Author(s) 2026. CC BY 4.0 License.


When combined with the EFG framework, these time-dense observations provide the basis for operational early-warning systems that identify emerging risks and support timely interventions before ecological thresholds are crossed. For the latest version of FROM-GLC Plus (Yu et al., 2025), this satellite view is further strengthened by near-surface camera networks, which supply high-frequency phenological records across forests, grasslands, wetlands and croplands, linking canopy-scale functional dynamics to ground processes. These advances enable global monitoring to move beyond static assessments toward an integrated, observation-driven framework that can detect ecosystem change continuously and support more timely ecological risk assessment.

6 Data availability

The current working release of the annual terrestrial ecosystem maps for 1982-2024 can be accessed at https://doi.org/10.5281/zenodo.19448555 (Du et al., 2026), and can be accessed and viewed in Google Earth Engine at https://code.earthengine.google.com/74de9ae068d3c5a290b3feaf33dffcda. The FROM-GLC Plus land-cover data can be accessed at https://code.earthengine.google.com/bfbd99948e782e049c309ed05a334051. WorldClim version 2 is available at https://www.worldclim.org/. Hammond landforms are available at http://esriurl.com/hammond. The Spatial Database of Planted Trees version 2.0 is available at https://doi.org/10.46830/writn.23.00073 and https://forobs.jrc.ec.europa.eu/GFT. IUCN EFG indicative distribution maps are available at https://doi.org/10.5281/zenodo.3546513.

7 Conclusions

This study provides annual global terrestrial ecosystem functional group (EFG) maps for 1982–2024 in a consistent 1 km fractional representation. The framework integrates annual FROM-GLC Plus land cover with climate regions, landforms, and an explicit crosswalk, producing 507 WTE types and 41 terrestrial EFGs together with three cross-realm categories (Freshwater, Marine-Terrestrial, and Marine-Freshwater-Terrestrial). Validation for 1985–2024 yielded a mean overall accuracy of 86.14 ± 0.47 %, while comparisons with existing global ecosystem maps showed broad spatial consistency. By extending EFG mapping from a static representation to a temporally continuous record, the dataset enables long-term assessment of ecosystem composition, distribution, and transitions at regional to global scales. The dataset provides an important resource for biodiversity assessment, ecosystem accounting, conservation planning, ecological restoration, and long-term global ecosystem monitoring.

Author contribution

LY conceived the study. ZD and LY developed the workflow and conducted the mapping. All authors contributed resources, interpreted the results, and reviewed the manuscript.

Competing interests

The authors declare that they have no conflict of interest.

https://doi.org/10.5194/essd-2026-791
Preprint. Discussion started: 9 November 2026
© Author(s) 2026. CC BY 4.0 License.



Financial support

This work was supported by the National Key R&D Program of China (2024YFF1307600), the Technology Innovation Center for South China Sea Remote Sensing, Surveying and Mapping Collaborative Application, Ministry of Natural Resources (RSSMCA-2025-B006), the Liaoning Young Elite Scientists Sponsorship Program, and the Dalian Young Star of Science and Technology Project.

References

Affinito, F., Butchart, S. H. M., Nicholson, E., Hirsch, T., Williams, J. M., Campbell, J. E., Ferrari, M. F., Gabay, M., Gorini, L., Kalamujic Stroil, B., Kohsaka, R., Painter, B., Pinto, J. C., Scholz, A. H., Straza, T. R. A., Tshidada, N., Vallecillo, S., Widdicombe, S., and Gonzalez, A.: Assessing coverage of the monitoring framework of the Kunming-Montreal Global Biodiversity Framework and opportunities to fill gaps, Nat. Ecol. Evol., 9, 1280-1294, https://doi.org/10.1038/s41559-025-02718-3, 2025.

Asamoah, E. F., Beaumont, L. J., and Maina, J. M.: Climate and land-use changes reduce the benefits of terrestrial protected areas, Nature Climate Change, 11, 1105–1110, https://doi.org/10.1038/s41558-021-01223-2, 2021.

Bousfield, C. G., and Edwards, D. P.: The pan-tropical age distribution of regenerating tropical moist forest, Nat. Ecol. Evol., 9, 1205-1213, https://doi.org/10.1038/s41559-025-02721-8, 2025.

Carpenter, S. R., DeFries, R., Dietz, T., Mooney, H. A., Polasky, S., Reid, W. V., and Scholes, R. J.: Millennium Ecosystem Assessment: Research Needs, Science, 314, 257-258, https://doi.org/10.1126/science.1131946, 2006.

Cavender-Bares, J., Schneider, F. D., Santos, M. J., Armstrong, A., Carnaval, A., Dahlin, K. M., Fatoyinbo, L., Hurtt, G. C., Schimel, D., Townsend, P. A., Ustin, S. L., Wang, Z., and Wilson, A. M.: Integrating remote sensing with ecology and evolution to advance biodiversity conservation, Nat. Ecol. Evol., 6, 506-519, https://doi.org/10.1038/s41559-022-01702-5, 2022.

CBD: Kunming-Montreal Global Biodiversity Framework, https://www.cbd.int/gbf (last access: 13 September 2026), 2024.

Chen, C., Park, T., Wang, X., Piao, S., Xu, B., Chaturvedi, R. K., Fuchs, R., Brovkin, V., Ciais, P., Fensholt, R., Tømmervik, H., Bala, G., Zhu, Z., Nemani, R. R., and Myneni, R. B.: China and India lead in greening of the world through land-use management, Nature Sustainability, 2, 122–129, https://doi.org/10.1038/s41893-019-0220-7, 2019.

Colglazier, W.: Sustainable development agenda: 2030, Science, 349, 1048-1050, https://doi.org/10.1126/science.aad2333, 2015.

Conradi, T., Eggli, U., Kreft, H., Schweiger, A. H., Weigelt, P., and Higgins, S. I.: Reassessment of the risks of climate change for terrestrial ecosystems, Nat. Ecol. Evol., 8, 888-900, https://doi.org/10.1038/s41559-024-02333-8, 2024.

Csillik, O., Keller, M., Longo, M., Ferraz, A., Pinagé, E. R., Görgens, E. B., Ometto, J. P., Silgueiro, V., Brown, D., Duffy, P., Cushman, K. C., and Saatchi, S.: A large net carbon loss attributed to anthropogenic and natural disturbances in the

https://doi.org/10.5194/essd-2026-791
Preprint. Discussion started: 9 November 2026
© Author(s) 2026. CC BY 4.0 License.



Amazon Arc of Deforestation, Proceedings of the National Academy of Sciences of the United States of America, 121, e2310157121, https://doi.org/10.1073/pnas.2310157121, 2024.

Du, Z., & Yu, L. Global annual ecosystem functional groups (EFGs) from 1982 to 2024 [Dataset]. Zenodo. https://doi.org/10.5281/zenodo.19448555, 2026.

Du, Z., Yu, L., Yang, J., Xu, Y., Chen, B., Peng, S., Zhang, T., Fu, H., Harris, N., and Gong, P.: A global map of planting years of plantations, Sci. Data, 9, 141, https://doi.org/10.1038/s41597-022-01260-2, 2022.

Du, Z., Yu, L., Arvor, D., Li, X., Cao, X., Zhong, L., Zhao, Q., Ma, X., Wang, H., Liu, X., Zhang, M., Xu, B., and Gong, P.: Dual Data- and Knowledge-Driven Land Cover Mapping Framework for Monitoring Annual and Near-Real-Time Changes, IEEE T. Geosci. Remote, 62, 1-14, https://doi.org/10.1109/TGRS.2024.3430981, 2024.

ESA: Land Cover CCI Product User Guide Version 2.0, http://maps.elie.ucl.ac.be/CCI/viewer/download/ESACCI-LC-Ph2-PUGv2_2.0.pdf (last access: 13 September 2026), 2017.

Fick, S. E., and Hijmans, R. J.: WorldClim 2: new 1-km spatial resolution climate surfaces for global land areas, Int. J. Climatol., 37, 4302-4315, https://doi.org/10.1002/joc.5086, 2017.

Franco, M. A., Rizzo, L. V., Teixeira, M. J., Artaxo, P., Azevedo, T., Lelieveld, J., Nobre, C. A., Pöhlker, C., Pöschl, U., Shimbo, J., Xu, X., and Machado, L. A. T.: How climate change and deforestation interact in the transformation of the Amazon rainforest, Nature Communications, 16, 7944, https://doi.org/10.1038/s41467-025-63156-0, 2025.

Gong, P., Wang, J., Yu, L., Zhao, Y., Zhao, Y., Liang, L., Niu, Z., Huang, X., Fu, H., Liu, S., Li, C., Li, X., Fu, W., Liu, C., Xu, Y., Wang, X., Cheng, Q., Hu, L., Yao, W., Zhang, H., Zhu, P., Zhao, Z., Zhang, H., Zheng, Y., Ji, L., Zhang, Y., Chen, H., Yan, A., Guo, J., Yu, L., Wang, L., Liu, X., Shi, T., Zhu, M., Chen, Y., Yang, G., Tang, P., Xu, B., Giri, C., Clinton, N., Zhu, Z., Chen, J., and Chen, J.: Finer resolution observation and monitoring of global land cover: first mapping results with Landsat TM and ETM+ data, Int. J. Remote Sens., 34, 2607-2654, https://doi.org/10.1080/01431161.2012.748992, 2013.

Gorelick, N., Hancher, M., Dixon, M., Ilyushchenko, S., Thau, D., and Moore, R.: Google Earth Engine: Planetary-scale geospatial analysis for everyone, Remote Sens. Environ., 202, 18-27, https://doi.org/10.1016/j.rse.2017.06.031, 2017.

Heijmans, M. M. P. D., Magnússon, R. Í., Lara, M. J., Frost, G. V., Myers-Smith, I. H., van Huissteden, J., Jorgenson, M. T., Fedorov, A. N., Epstein, H. E., Lawrence, D. M., and Limpens, J.: Tundra vegetation change and impacts on permafrost, Nature Reviews Earth & Environment, 3, 68–84, https://doi.org/10.1038/s43017-021-00233-0, 2022.

Karagulle, D., Frye, C., Sayre, R., Breyer, S., Aniello, P., Vaughan, R., and Wright, D.: Modeling global Hammond landform regions from 250-m elevation data, T. GIS, 21, 1040-1060, https://doi.org/10.1111/tgis.12265, 2017.

Keith, D. A., Ferrer-Paris, J. R., Nicholson, E., Bishop, M. J., Polidoro, B. A., Ramirez-Llodra, E., Tozer, M. G., Nel, J. L., Mac Nally, R., Gregr, E. J., Watermeyer, K. E., Essl, F., Faber-Langendoen, D., Franklin, J., Lehmann, C. E. R., Etter, A., Roux, D. J., Stark, J. S., Rowland, J. A., Brummitt, N. A., Fernandez-Arcaya, U. C., Suthers, I. M., Wiser, S. K.,

https://doi.org/10.5194/essd-2026-791
Preprint. Discussion started: 9 November 2026
© Author(s) 2026. CC BY 4.0 License.



Donohue, I., Jackson, L. J., Pennington, R. T., Iliffe, T. M., Gerovasileiou, V., Giller, P., Robson, B. J., Pettorelli, N., Andrade, A., Lindgaard, A., Tahvanainen, T., Terauds, A., Chadwick, M. A., Murray, N. J., Moat, J., Pliscoff, P., Zager, I., and Kingsford, R. T.: A function-based typology for Earth's ecosystems, Nature, 610, 513-518, https://doi.org/10.1038/s41586-022-05318-4, 2022.

Lehner, B., Beames, P., Mulligan, M., Zarfl, C., De Felice, L., van Soesbergen, A., Thieme, M., Garcia de Leaniz, C., Anand, M., Belletti, B., Brauman, K. A., Januchowski-Hartley, S. R., Lyon, K., Mandle, L., Mazany-Wright, N., Messager, M. L., Pavelsky, T., Pekel, J.-F., Wang, J., Wen, Q., Wishart, M., Xing, T., Yang, X., and Higgins, J.: The Global Dam Watch database of river barrier and reservoir information for large-scale applications, Sci. Data, 11, 1069, https://doi.org/10.1038/s41597-024-03752-9, 2024.

Li, C., Gong, P., Wang, J., Zhu, Z., Biging, G. S., Yuan, C., Hu, T., Zhang, H., Wang, Q., Li, X., Liu, X., Xu, Y., Guo, J., Liu, C., Hackman, K. O., Zhang, M., Cheng, Y., Yu, L., Yang, J., Huang, H., and Clinton, N.: The first all-season sample set for mapping global land cover with Landsat-8 data, Sci. Bull., 62, 508-515, https://doi.org/10.1016/j.scib.2017.03.011, 2017.

Meyer, H., and Pebesma, E.: Machine learning-based global maps of ecological variables and the challenge of assessing them, Nat. Commun., 13, 2208, https://doi.org/10.1038/s41467-022-29838-9, 2022.

Murray, N. J., Buschke, F., Cresswell, B. J., Gros-Dubois, N., Keith, D., Lloyd, T. J., Meyer, C., Young, A. R., Askay, S., Azevedo, T., Bajwa, M., Birch, T., Breyer, S., Burgess, N. D., Campbell, J., Canto, R. F., Dayaram, A., Driver, A., Filipp, R., Frye, C., Gomersall, L., Harmer, T., Hughes, A. C., Jetz, W., Lambertini, M., Lucas, R., Lynn, A., Masson, W. D., Moore, R., Moncrieff, G., Narayan, D., Nicholson, E., Otterlee, M., Paganini, M., Pasquarella, V. J., Patterson, D., Redmon, J., Saunders, R., Schechter, E., Sims, M. J., Skowno, A., Smets, B., Steer, B. S. C., Valderrabano, M., Venturini, S., and Gevorgyan, Y.: The Global Ecosystems Atlas: comprehensive and systematic mapping of Earth's ecosystems, manuscript dated 16 July 2026, 2026.

Nicholson, E., Andrade, A., Brooks, T. M., Driver, A., Ferrer-Paris, J. R., Grantham, H., Gudka, M., Keith, D. A., Kontula, T., Lindgaard, A., Londono-Murcia, M. C., Murray, N., Raunio, A., Rowland, J. A., Sievers, M., Skowno, A. L., Stevenson, S. L., Valderrabano, M., Vernon, C. M., Zager, I., and Obura, D.: Roles of the Red List of Ecosystems in the Kunming-Montreal Global Biodiversity Framework, Nat. Ecol. Evol., 8, 614-621, https://doi.org/10.1038/s41559-023-02320-5, 2024.

Olofsson, P., Foody, G. M., Herold, M., Stehman, S. V., Woodcock, C. E., and Wulder, M. A.: Good practices for estimating area and assessing accuracy of land change, Remote Sens. Environ., 148, 42–57, https://doi.org/10.1016/j.rse.2014.02.015, 2014.

Richardson, K., Steffen, W., Lucht, W., Bendtsen, J., Cornell, S. E., Donges, J. F., Drüke, M., Fetzer, I., Bala, G., von Bloh, W., Feulner, G., Fiedler, S., Gerten, D., Gleeson, T., Hofmann, M., Huiskamp, W., Kummu, M., Mohan, C., Nogués-Bravo, D., Petri, S., Porkka, M., Rahmstorf, S., Schaphoff, S., Thonicke, K., Tobian, A., Virkki, V., Wang-Erlandsson,

https://doi.org/10.5194/essd-2026-791
Preprint. Discussion started: 9 November 2026
© Author(s) 2026. CC BY 4.0 License.



L., Weber, L., and Rockström, J.: Earth beyond six of nine planetary boundaries, Sci. Adv., 9, eadh2458, https://doi.org/10.1126/sciadv.adh2458, 2023.

Richter, J., Goldman, E. D., Harris, N. L., Gibbs, D. A., Rose, M. A., Peyer, S. M., Richardson, S., and Velappan, H.: Spatial Database of Planted Trees (SDPT Version 2.0), World Resources Institute [data set], https://doi.org/10.46830/writn.23.00073, 2024.

Riggio, J., Baillie, J. E., Brumby, S., Ellis, E., Kennedy, C. M., Oakleaf, J. R., Tait, A., Tepe, T., Theobald, D. M., Venter, O., Watson, J. E. M., Jacobson, A. P. Global human influence maps reveal clear opportunities in conserving Earth's remaining intact terrestrial ecosystems. Glob Change Biol. 2020; 26: 4344–4356. https://doi.org/10.1111/gcb.15109

Sayre, R., Karagulle, D., Frye, C., Boucher, T., Wolff, N. H., Breyer, S., Wright, D., Martin, M., Butler, K., Van Graafeiland, K., Touval, J., Sotomayor, L., McGowan, J., Game, E. T., and Possingham, H.: An assessment of the representation of ecosystems in global protected areas using new maps of World Climate Regions and World Ecosystems, Global Ecol. Conserv., 21, e00860, https://doi.org/10.1016/j.gecco.2019.e00860, 2020.

Schmidt-Traub, G.: National climate and biodiversity strategies are hamstrung by a lack of maps, Nat. Ecol. Evol., 5, 1325-1327, https://doi.org/10.1038/s41559-021-01533-w, 2021.

Sides, K. B., Naji, N., Kremer, A., Burton, D., and Sayre, R.: A crosswalk of the 2015 World Terrestrial Ecosystems to the International Union for Conservation of Nature Global Ecosystem Typology Framework, U.S. Geological Survey Open-File Report 2025-1043, 10 pp., https://doi.org/10.3133/ofr20251043, 2025.

Song, X.-P.: The future of global land change monitoring, Int. J. Digit. Earth, 16, 2279-2300, https://doi.org/10.1080/17538947.2023.2224586, 2023.

Sulla-Menashe, D., Gray, J. M., Abercrombie, S. P., and Friedl, M. A.: Hierarchical mapping of annual global land cover 2001 to present: The MODIS Collection 6 Land Cover product, Remote Sens. Environ., 222, 183-194, https://doi.org/10.1016/j.rse.2018.12.013, 2019.

Theobald, D. M., Oakleaf, J. R., Moncrieff, G., Voigt, M., Kiesecker, J., and Kennedy, C. M.: Global extent and change in human modification of terrestrial ecosystems from 1990 to 2022, Sci. Data, 12, 606, https://doi.org/10.1038/s41597-025-04892-2, 2025.

UNCCD: World atlas of desertification, https://www.unccd.int/resources/reports/world-atlas-desertification (last access: 13 September 2026), 2022.

Yu, L., Du, Z., Dong, R., Zheng, J., Tu, Y., Chen, X., Hao, P., Zhong, B., Peng, D., Zhao, J., Li, X., Yang, J., Fu, H., Yang, G., and Gong, P.: FROM-GLC Plus: toward near real-time and multi-resolution land cover mapping, GISci. Remote Sens., 59, 1026-1047, https://doi.org/10.1080/15481603.2022.2096184, 2022.

Yu, L., Du, Z., Li, X., Gu, J., Li, X., Zhong, L., Duojiweise, Wu, H., Zhao, Q., Ma, X., Zheng, J., Yang, Y., Song, W., Wang, P., Zhao, Z., Liao, L., Long, Y., Zhang, Y., Peng, J., Shen, M., Li, T., Sun, Z., Zhao, Y., Wu, C., Lin, G., Luo, Y.,

https://doi.org/10.5194/essd-2026-791
Preprint. Discussion started: 9 November 2026
© Author(s) 2026. CC BY 4.0 License.



547 and Peng, D.: FROM-GLC Plus 3.0: Multimodal Land Change Mapping with SAM and Dense Surface Observations, J.
548 Remote Sens., 5, 0728, https://doi.org/10.34133/remotesensing.0728, 2025.

549 Zeng, Y., Hao, D., Huete, A., Dechant, B., Berry, J., Chen, J. M., Joiner, J., Frankenberg, C., Bond-Lamberty, B., Ryu, Y.,
550 Xiao, J., Asrar, G. R., and Chen, M.: Optical vegetation indices for monitoring terrestrial ecosystems globally, Nat. Rev.
551 Earth Environ., 3, 477-493, https://doi.org/10.1038/s43017-022-00298-5, 2022.

552 Zhang, X., Zhao, T., Xu, H., Liu, W., Wang, J., Chen, X., and Liu, L.: GLC_FCS30D: the first global 30 m land-cover
553 dynamics monitoring product with a fine classification system for the period from 1985 to 2022 generated using dense-
554 time-series Landsat imagery and the continuous change-detection method, Earth Syst. Sci. Data, 16, 1353-1381,
555 https://doi.org/10.5194/essd-16-1353-2024, 2024.